4th IAA Planetary Defense Conference – PDC 2015
13-17 April 2015, Frascati, Roma, Italy

IAA-PDC-15-P-42

DETECTION PERFORMANCE OF L1-BASED NEO SURVEYS

Philipp Maier[1], Raffaella Franco[2], Johannes Gelhaus[3] , and Sven Müller[4]
[1]ESA/ESTEC, Keplerlaan 1, NL-2200 AZ, Noordwijk, The Netherlands, +31 71 565 3147, philipp.maier@esa.int
[2]ESA/ESTEC, Keplerlaan 1, NL-2200 AZ, Noordwijk, The Netherlands, +31 71 565 4772, raffaella.franco@esa.int
[3]Technische Universität Braunschweig, Hermann-Blenk-Str. 23, 38108 Braunschweig, Germany, johannes.gelhaus@dlr.de
[4] Technische Universität Braunschweig, Hermann-Blenk-Str. 23, 38108 Braunschweig, Germany, +49 531 391-9974, sv.mueller@tu-braunschweig.de

Keywords: *neo survey, space-based, detection performance, L1, telescope*

Abstract
Ground-based near-Earth object surveys bear intrinsic limitations in terms of observation time and observational biases. Space-based asteroid surveys, while perceived as much more costly, offer a valuable complement in regards to observation time and observable sky regions. The highly successful NEOWISE project is a prime example.
A considerable increase in data from space-based observations could be achieved if it was possible to gain value-adding data with compact sensors or with devices already installed on spacecraft. For a hypothetic space environment mission on an orbit around L1 we thus investigate and compare the expected detection performance of different instruments with a mass of less than 3 kg each. The considered sensors range from a field of view of 5x5 square degrees to 140x140 square degrees and limiting magnitudes from 16 to 9 respectively.
As reference population, the outcome of the newly developed near-Earth object population model by Granvik, Morbidelli, Bottke, and collaborators is used, with more than 25,000 objects at absolute magnitudes of 22 and brighter. Calculations are performed using the ESA NEOPOP population analysis and observation simulation tool.

1. Introduction
Space based asteroid surveys offer various advantages that make them valuable complements to ground based observations. The observational geometry and the location outside of the atmosphere allow for longer observation times. The missing atmosphere allows for observations in the infrared spectral range in addition to the visible range. In addition, the observational geometry especially of sensors on orbits interior to Earth's orbit favor the observation of near-Earth objects (NEOs) with different orbital properties compared to ground based sensors. Among those are prominently interior to Earth orbit objects (IEOs), of which currently only a small fraction (about 3% of those at absolute magnitude 22 or brighter) of the estimated total is known due to an unfavorable observation geometry from Earth.

The NEOWISE survey is a prime example of such a space based mission, with 135 previously unknown NEOs discovered during 13 months of primary survey duration (Mainzer, et al., 2011). The instrument used in this case was the 40 cm aperture infrared telescope of the WISE spacecraft, located in a sun-synchronous Earth orbit with 525 km of altitude (National Aeronautics and Space Administration, 2010).
Proposals have also been made to use smaller instruments or even instruments already present on many spacecraft, such as star trackers, in the visible spectral range for non-dedicated surveys (Svedhem & Koschny, 2012). While the discovery rates of single sensors in such an approach would be much lower compared to larger missions, the cost would be significantly lower and a larger number of instruments on different spacecraft could partly compensate for the weaker individual performance.
Following this approach, we thus investigate the potential performance of small sensors in the visible spectral range placed on a hypothetical space weather spacecraft in an orbit around the Sun-Earth L1 point.

2. NEOPOP – Near Earth Object Analysis and Observation Simulation Tool[1]

The European Space Agency's (ESA) Near-Earth Object Analysis and Observation Simulation Tool (NEOPOP) was used to conduct the main part of the analysis at hand.
NEOPOP is a software tool that allows for the generation, analysis, and visualization of NEO populations on the one hand, and for the simulation and analysis of observations on the other hand.
For the generation of NEO populations, it includes a new NEO model developed by Granvik, Morbidelli, Bottke and collaborators. The model follows the approach of the original Bottke model (Bottke, Jedicke, Morbidelli, Petit, & Gladman, 2000), but is improved concerning the number of source regions assumed for NEOs (seven instead of five), the perturbing effects on NEO orbits considered, and, most notably, the number of observations used to calibrate the model.
The observation simulation part of NEOPOP includes a detailed performance model for optical sensors in the visible and infrared bands, and a basic performance model for mono- and bistatic radar sensors. It allows both space and ground based observations with either simple viewing directions or detailed pointing plans.
For the study at hand, the detailed technical properties were only known for two of the sensors considered. Due to this, the sensors were not modelled in detail using NEOPOP's optical performance model. Instead, the crossing geometry and lighting conditions were calculated using NEOPOP and the detectability decision was made using estimated limiting magnitudes for each sensor.

3. Considered Sensors and their Simulation

In the context of the hypothetical L1-mission, a mass envelope of 3 kg was assumed to be available for a NEO instrument. In order to allow a trade-off between field-of-view (FoV) and limiting magnitude, three different sensors of approximately this instrument mass were considered. Their observational performance parameters are documented in table 1. All three instruments work in the visible spectrum range, thus greatly reducing necessary efforts to cool the sensor compared to observations in the thermal infrared spectral region.

[1] For more details, see the final report of the SGNEOP project, (Gelhaus, Hahn, Müller, & Franco, 2015)

	SPOSH (SP)	Terma Star Tracker (ST)	Telecam (TC)
FoV [deg²]	140x140	22x22	5x5
Limiting magnitude [mag]	9	14	16
Aperture diam. [mm]	6.5	22	50

Table 1 Simulated sensors

SPOSH refers to the Smart Panoramic Optical Sensor Head (SPOSH), a wide field-of-view instrument originally developed for meteor detections by the German Aerospace Center and Jena-Optronik under a contract from ESA. Camera breadboards have been built and tested and a design of a flight model has been developed. The ground-based breadboard tests showed that the camera could detect meteors with apparent magnitudes down to $m_v = 6$ at exposure times of 0.06 s. (Oberst, et al., 2011) Estimates show, however, that with longer observation times feasible for asteroid surveys, a limiting magnitude of $m_v = 9$ should be achievable. In addition, an increased field of view of 140x140 deg² instead of 120x120 deg² for the original SPOSH concept was assumed.
The Terma Star Tracker represents the commercially available star tracker HE-5AS as manufactured by Terma (Terma A/S Space, 2012). This sensor is already being flown on several satellites, including ESA's Cryosat 2. If observations with this sensor prove feasible, an additional advantage would be that flying sensors on different spacecraft could be used part-time for NEO surveys. Estimates show that a limiting magnitude for asteroid observations of $m_v = 14$ can be achieved.
The Telecam instrument shall represent a smaller field-of-view instrument capable of imaging fainter objects. It is loosely based on the NAVCAM navigation camera on board the Rosetta spacecraft, with an estimated limiting magnitude of $m_v = 16$.

Since NEOPOP does not allow FoVs larger than 10x10 deg², the two sensors with larger FoVs had to be simulated differently. The Terma Star Tracker FoV was simulated as 16 sensors with a FoV of 5.5x5.5 deg² each.
For the SPOSH sensor, a simulation with the entire field of view would have taken an excessive amount of computing time. Especially the results of sensor TC showed, however, that detections and crossings occurred predominantly close to the ecliptic. The higher likelihood of detections in this area can be explained mainly by the larger density of objects in this region. Since observation conditions become even more important for a sensor with a smaller limiting magnitude, it is reasonable to assume that the SPOSH sensor will – if any – detect most objects close to the ecliptic. Thus, the simulation of the SPOSH sensor was limited to 28 sub-sensors of 10x10 deg² FoV each, pointing close to the ecliptic. This results in a FoV of 140x20 deg².

4. Simulated Orbit and Pointing Directions

Since, at the time this analysis was conducted, NEOPOP only allowed for keplerian orbits (including movement of the line of nodes and the line of apsides), a true orbit around L1 could not be simulated. Instead, the orbit of L1 was approximated via a keplerian orbit. This causes small deviations from a true orbit around L1 over time, resulting in an orbit duration of 355 days. While this does not change the observation geometry dramatically, it affects pointing directed "behind" the Earth, since Earth in this case crosses the FoV over time due to the sensor's faster heliocentric motion.

In order to also allow for a comparison of different installation points of the camera on the spacecraft, five different pointing directions from L1 were considered as described in table 2 (see also Figure 1).

Scenario	***Pointing Direction***
1	centered on Earth
2	20 deg off-pointing from Sun-Earth vector
3	90 deg off-pointing from Sun-Earth vector in the ecliptic
4	90 deg off-pointing from Sun-Earth vector perpendicular to the ecliptic
5	150 deg off-pointing from the Sun-Earth vector (i.e. towards the sun)

Table 2: Simulated pointing directions

In scenarios 2 and 5, different numbers of NEOs can be expected to cross the FoV depending on whether the off-pointing takes place within the ecliptic or to a direction outside of the ecliptic. The effect is especially to be expected for instruments with a small FoV. For this reason, three sub-scenarios are introduced for pointing scenario 2: 20 degrees off-pointing within the ecliptic in the orbital velocity direction of Earth, and 20 degrees off-pointing perpendicular to the ecliptic, North and South. They are numbered 2a, 2b, and 2d, respectively. An off-pointing within the ecliptic against the orbital velocity direction of Earth (hypothetical scenario 2c) would lead to falsified results due to the Earth crossing the sensor's FoV over time.

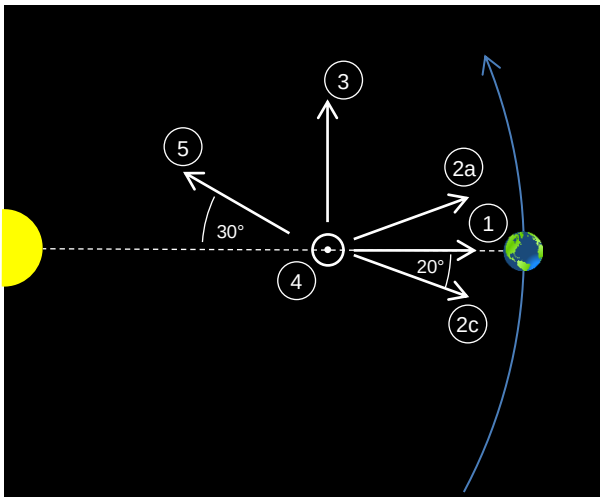

Figure 1: Simulated sensor pointing directions

Due to the different orbital periods around the sun, the effect of the Earth blocking part of the FoV in scenario 1 is not accounted for. Equally, the weaker expected observational performance due to stray light of the Earth in this scenario is not taken into account.

To decrease the computation effort especially for the SPOSH sensor, not all scenarios were simulated. With its large FoV of 140x140 deg², the observed area of the 2a, 2b, and 2d sub-scenarios largely overlap. Especially in the case of 2b and 2d only areas at high absolute values of ecliptic latitudes change, where the probability of detections is considered low. For this reason, scenarios 2b and 2d are not simulated with the SPOSH sensor. Equally, scenario 5 is not simulated with SPOSH

since at this orientation, the sun would be inside the sensor's FoV at all times. Scenario 4 is omitted for SPOSH based on the worse results for this scenario shown by the other sensors and a large overlap with scenario 3.

5. Underlying NEO Population

The population used was created based on the 2015 NEO population model of Granvik, Morbidelli, Bottke, and collaborators included in NEOPOP (Gelhaus, Hahn, Müller, & Franco, 2015). For an absolute magnitude range between 5 and 22, this model predicts 25,653 objects, which were used for the simulation. As figure 2 shows, among these are 412 especially interesting Atira objects. Figure 3 furthermore shows the distribution of absolute magnitude for the source population.

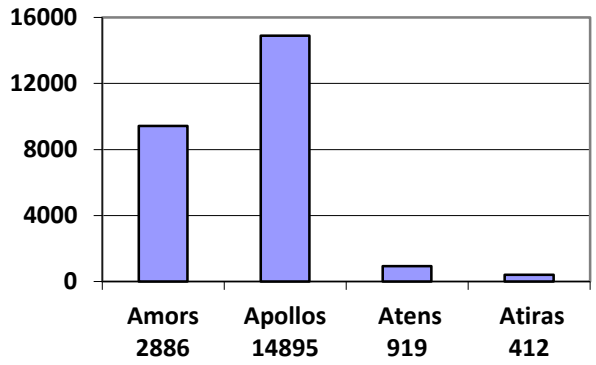

Figure 2 NEO population group distribution

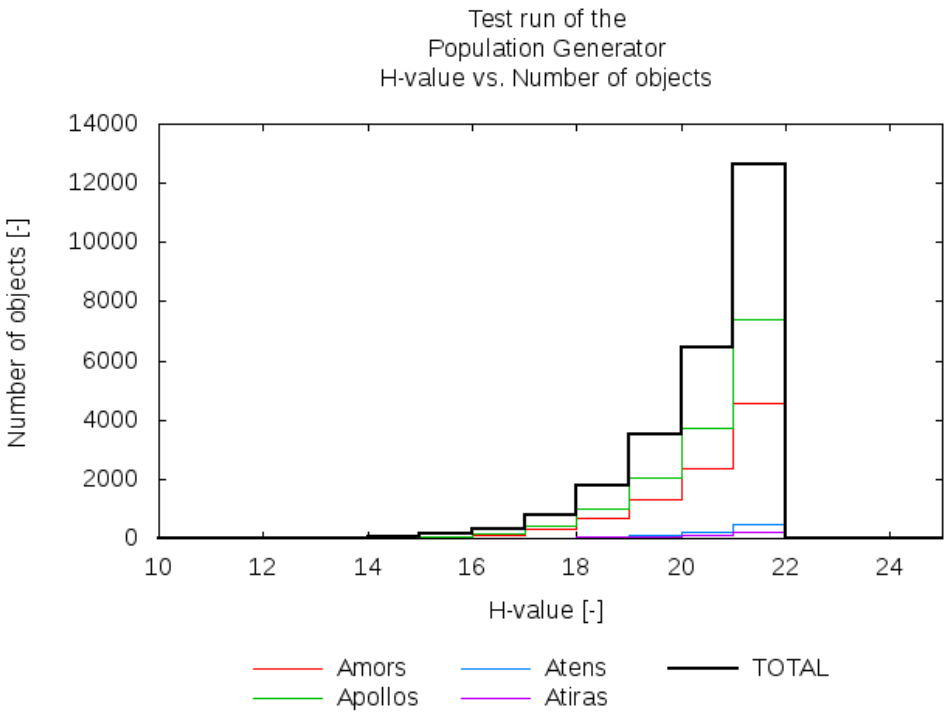

Figure 3 Absolute magnitude distribution of used NEO population

6. Results

In order to achieve meaningful results and to minimize the bias of initial orbital positions of the individual objects, each sensor and viewing direction was simulated over 10 years and 99 Monte Carlo runs were carried out for each scenario.

Table 3 shows the preliminary results of simulated observations on the modelled NEO population using the sensors with their described default characteristics. The detection decision was made based on whether an object had an apparent magnitude equal to or brighter than the sensor's limiting magnitude at the time of crossing the sensor's FoV. Multiple detections of the same object were not counted as separate detections. These results already clearly show that the larger field of view of SPOSH cannot compensate the weaker sensitivity for faint objects. For all pointing directions but direction 1, the simulations also show a slightly better performance of the more sensitive Telecam compared to the Star Tracker. At these close-to-optimum phase angles, the cut of the modelled population at H = 22 probably leads to an underestimation of the objects detectable by the Telecam.

Detected objects in modelled population (10 years)								
Sensor Lim. M	***Scenario:***	***1***	***2a***	***2b***	***2d***	***3***	***4***	***5***
SP	Mean	0.3	0.3			0.1		
9	*StdDev*	*0.5*	*0.5*			*0.3*		
ST	Mean	17.6	12.2	11.3	13.2	7.9	5.7	8.9
14	*StdDev*	*3.7*	*3.2*	*3.1*	*3.1*	*2.4*	*2.4*	*1.3*
TC	Mean	17.3	16.6	14.3	15.1	12.8	5.8	18.6
16	*StdDev*	*4.3*	*3.8*	*4.0*	*3.9*	*3.4*	*2.5*	*2.7*

Table 3: Mean numbers of detected objects in the modelled NEO population over 10 years

The results also confirm the expected better performance in scenarios that combine small phase angles with small potential observation distances (i.e. 1, 2a, 2b, 2d) over others. The only notable exception is scenario 5, especially for the more sensitive Telecam. A closer observation of the data reveals that in this case, most objects were observed at phase angles smaller than 80 deg and at observational ranges in between 0.8 and 1.4 AU, i.e. "on the other side" of the sun. A further look also shows that most of these objects were within the orbit of Venus at the time of observation. The results furthermore confirm the advantage of pointing in or close to the ecliptic, as the weak results of scenario 4 show. An off-pointing of 20 deg, as applied in scenarios 2b and 2d, proves to be still acceptable, though, and only shows a tendency towards a small decrease in detectable objects.

Since the focus of this paper is on surveys, it is furthermore of prime interest to assess the likelihood of the observed objects being newly discovered objects. This was done in two ways: firstly, the same observations as performed on the modelled population were carried out again on the population included in the catalogue of known Near-Earth Asteroids provided by the Minor Planet Center (status of September 22nd, 2014). Comparing the results of the two simulation campaigns provides an indication of how many of the detected objects are likely to be known already.

Secondly, the orbital properties of the detected objects are examined in order to assess whether it is likely to detect objects belonging to a sparsely known subgroup, such as interior to Earth orbit objects.

The first approach, the observation simulation on the population of known NEOs, was only carried out for the two sensors with generally good detection performance, i.e. sensors ST and TC. The results of this simulation were then subtracted from the results of the observation simulation on the modelled population to provide an estimate of the number of new objects likely to be discovered (without taking into account future discoveries until the potential launch date). Table 4 shows the results of this examination.

Estimate of new discoveries (10 years)								
Sensor Lim. M	**Scenario:**	**1**	**2a**	**2b**	**2d**	**3**	**4**	**5**
ST 14		0.3	0.0	0.0	1.1	0.0	1.2	1.5
TC 16		1.5	1.6	0.1	1.7	1.2	1.6	0.6

Table 4: Differences between detected objects in modelled population and detected objects in population of known NEOs over 10 years

Two aspects of the results are particularly noteworthy: firstly, the evaluation shows that the estimated number of new discoveries is notably higher with the Telecam. This is in line with the expectation that a more sensitive sensor would detect more of the less known population of fainter objects. Secondly, scenario 5, which showed the largest number of overall detectable objects, now shows considerably less potential new discoveries than most other scenarios. The reason being that due to the large phase angles in scenario 5, most objects are detected in the absolute magnitude range between 14 and 17. In scenario 1, for example, many more faint objects are detected, as figure 4 shows.

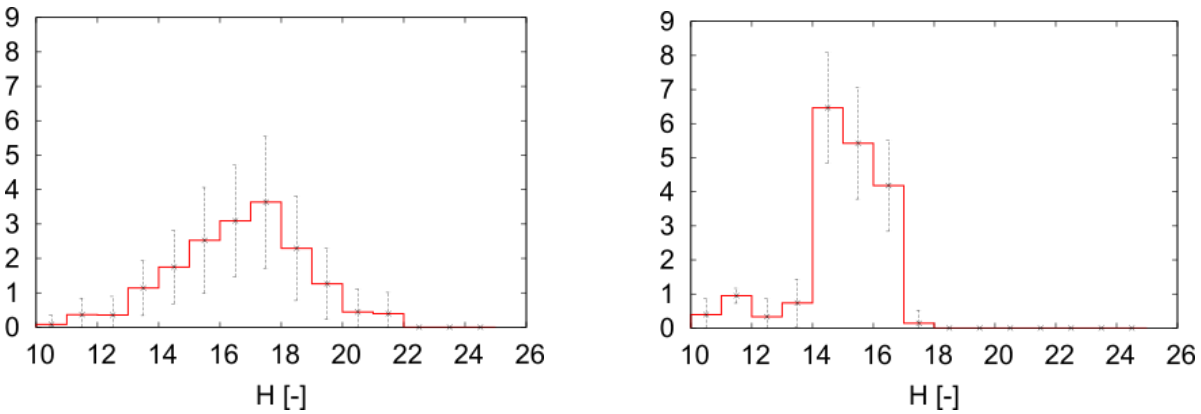

Figure 4: Absolute magnitude distributions of detected objects in bins of 1. For Telecam scenario 1 (left) and Telecam scenario 5 (right).

Examining the distribution of orbital elements shows clear tendencies towards less detections of Atens and more detections of Amors when moving the pointing direction from sun-directed to the outer solar system (i.e. from scenario 5 to scenario 1). This is in line with the expectations. Comparing the Telecam and the Star Tracker, a smaller number of detectable Amors can be noticed in the Star Tracker scenarios. This can be explained by the larger pericenter distances compared to the other NEO groups.

Both sensors, however, are expected to provide only very few new discoveries. It would thus be interesting to assess how the detections and potential discoveries

would improve if the sensor sensitivity was improved, if by larger apertures, longer exposure times, or other processing techniques. Table 5 therefore shows the expected numbers of detectable objects for sensors ST and TC under the assumption that their limiting magnitude could be improved by two magnitudes. Table 6 shows the expected number of new discoveries under the same assumption, calculated as described above.

Detected objects in modelled population (10 years, improved sensors)								
Sensor Lim. M	***Scenario:***	***1***	***2a***	***2b***	***2d***	***3***	***4***	***5***
ST	Mean	117.7	76.9	82.1	82.7	79.8	44.4	69.9
16	*StdDev*	*9.2*	*7.6*	*7.6*	*9.0*	*7.4*	*37.1*	*4.4*
TC	Mean	100.0	101.4	89.1	84.3	93.0	30.1	136.0
18	*StdDev*	*9.8*	*8.4*	*8.2*	*9.0*	*9.4*	*20.7*	*8.7*

Table 5: Mean numbers of detected objects in the modelled NEO population over 10 years for improved sensors

Estimate of new discoveries (10 years, improved sensors)								
Sensor Lim. M	**Scenario:**	**1**	**2a**	**2b**	**2d**	**3**	**4**	**5**
ST 16		20.4	13.6	13.0	13.5	7.6	15.5	2.6
TC 18		13.8	15.6	15.4	9.1	20.0	11.6	21.0

Table 6: Differences between detected objects in modelled population and detected objects in population of known NEOs over 10 years for improved sensors

These results for more sensitive sensors show that under the chosen conditions, the best choice of sensor would indeed depend on the most likely pointing direction. For example for viewing directions with close to optimal phase angles (scenario 1), the larger FoV instrument is advantageous. For scenario 4, the relative sparseness of objects crossing the sensor FoVs (605 for TC, 2806 for ST vs. 11247 for TC, 21440 for ST in scenario 3) also seems to favor the larger FoV instrument.

7. Conclusion

The simulations showed a relatively weak discovery performance for the original sensors that fitted the defined mass envelope. The results thus strongly suggest to employ more sensitive, but probably heavier, sensors in order to achieve a better survey performance if deployed as a single sensor. Within the scope of the originally considered values, they also indicate that an improvement in sensitivity should be preferred over an improvement in field of view.

Given the relatively low mass of the sensors, though, it might be worth to consider them as payloads distributed on several missions, or in case of the Star Trackers, to use flying hardware during otherwise idle time.

8. Bibliography

Bottke, W. F., Jedicke, R., Morbidelli, A., Petit, J., & Gladman, B. (2000). Understanding the Distribution of Near-Earth Asteroids. *Science*(288), 2190-2194.

Gelhaus, J., Hahn, G., Müller, S., & Franco, R. (2015). *Synthetic Generation of a NEO Population.* Final Report, ESA contract N. AO/1-7015/11/NL/LvH.

Mainzer, A., Grav, T., Bauer, J., Masiero, J., McMillan, R. S., Cutri, R. M., et al. (2011). NEOWISE Observations of Near-Earth Objects: Preliminary Results. *The Astrophysical Journal, 743*(2).

National Aeronautics and Space Administration. (2010). Wide-field Infrared Survey Explorer Fact Sheet. Retrieved March 04, 2015, from http://wise.ssl.berkeley.edu/documents/FactSheet.2010.1.4.pdf

Oberst, J., Flohrer, J., Elgner, S., Maue, T., Margonis, A., Schrödter, R., et al. (2011). The Smart Panoramic Optical Sensor Head (SPOSH) — A camera for observations of transient luminous event on planetary night sides. *Planetary and Space Science*(59), 1-9.

Svedhem, H., & Koschny, D. (2012). Searching for Interior to Earth Orbit Asteroids (IEO's) by Using Spacecraft Star Trackers. *Asteroids, Comets, Meteors.* Niigata, Japan.

Terma A/S Space. (2012, February). Star Tracker HE-5AS. Retrieved from http://www.terma.com/media/101677/star_tracker_he-5as.pdf